MEASUREMENT OF STATIC AND DYNAMIC FRICTION ENERGY ABSORPTION IN CARBON/VINYL ESTER COMPOSITE

Thomas J. Brimhall, PhD, PE

Altair Engineering

Abstract

Experiments have suggested that sliding friction plays an important role in the energy absorption of composite crush tubes. In an attempt to separate the sliding friction specific energy absorption, SEA, from the SEA attributable to matrix damage due to bending, an innovative strip testing fixture was designed, fabricated, and tested. With this fixture, strips of composite can be crushed under two fixture configurations; with and without sliding friction. The resulting load vs. deflection data is then analyzed to calculate SEA attributable to sliding friction.

Strips of braided carbon/vinyl ester composite were tested statically and dynamically. The relative SEA attributable to sliding friction, similar to that found when a tube is crushed with a plug type trigger, was measured. It was observed that matrix damage due to bending did not change significantly when loaded dynamically compared with the quasi-static result. Sliding friction SEA, however, did show significant decrease when loaded dynamically vs. the quasi-static result and accounts for nearly all of the difference in SEA between dynamic and quasi-static loading.

Introduction

Quantifying the sliding friction component of SEA requires a test that isolates friction. To accomplish this goal, a test fixture was proposed to test strips of composite material that would remove friction energy absorption from the crush process present when carbon composite is forced to slide over the steel surface of a crush trigger under quasi-static and dynamic load rates. The test fixture was designed to simulate the damage process present in the sides of a round cornered, square section crush tube when it is compressed using a plug trigger.

A schematic of the strip test fixture is presented in Figure 1. The main working parts are four rollers mounted in low friction ball bearings. Because rollers are supported by ball bearings, there is essentially no sliding friction present when the rollers rotate as the strip specimen is forced downward. Three guide rollers that support the test strip are of the same diameter, 12.7 mm, to simplify design and fabrication. The diameter of the three rollers was selected because the roller radius is similar to the 6 mm radius of the standard plug trigger used in the tube crush test and to keep the test fixture compact and minimize the length of the strip specimen. Rollers A and C are aligned in the vertical direction. The roller second from the top, roller B, is adjustable horizontally to accommodate varying thicknesses of samples. The lowest roller, roller D, is twice the diameter, 25.4 mm, of the other three rollers and, like roller B, is also horizontally adjustable. The larger diameter of roller D was chosen so that the range of curvature imposed on a strip test specimen could be varied over a large range by adjusting the horizontal position to simulate the curvature imposed on crush tubes when triggers with fillets of varying radii are used. Roller D is positioned to force the composite strip specimen to bend against the bottom guide roller, roller C, as the specimen is forced downward during testing.

Roller D was designed to have two test modes, locked and unlocked. When unlocked, roller D is free to rotate. When locked, roller D is prevented from rotating with a pin that fits into a hole in the roller that prevents the roller from rotating forcing the strip specimen to slide over roller D. The difference in the manner of loading between the unlocked and free mode is due only to the sliding friction present when roller D is kept from rotating, forcing the strip to slide over the surface of the roller D. Sliding friction is thus removed from the damage process when roller D is free. Delamination and matrix damage due to bending are present when roller D is locked or free.

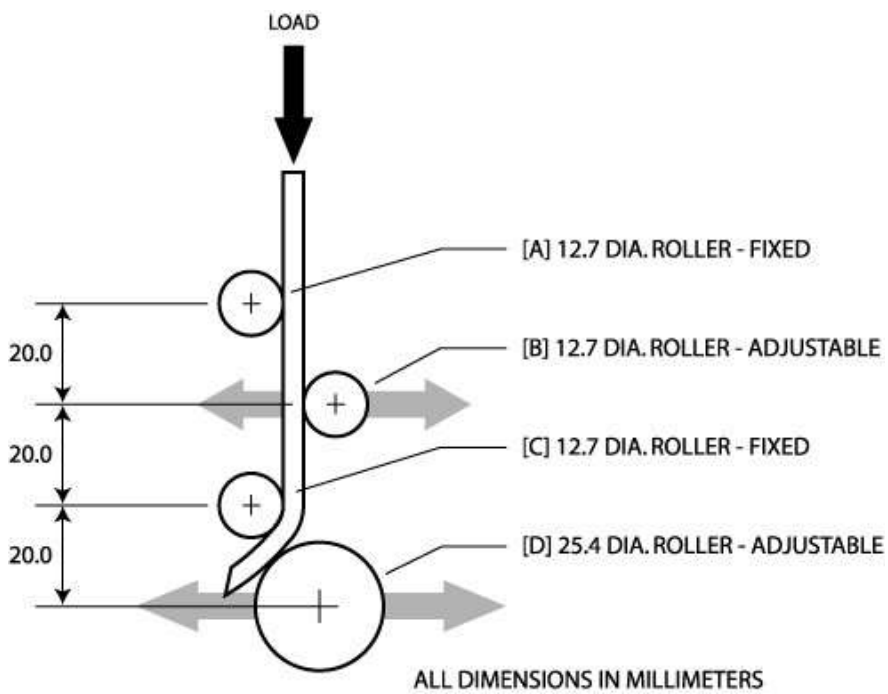

Figure 1 Strip test fixture schematic.

Strip Test Specimen and Fixture Description

Test specimens were machined from a four ply, flat plaque 4.0 mm thick. Plaque layup description is presented in Table I and mechanical properties are presented in Table II. A schematic of the braided fiber architecture is presented in Figure 2.

Table 1 Composite plaque characteristics.

Reinforcement	Matrix	Architecture	Fiber Content (wt. %)	Fiber Volume (%)	Laminate Density (gm/cm^3)
Carbon Fiber Fortafil 503 80k Axial Grafil 12k Off-Axis	Ashland Hetron 922 Vinyl Ester	Tri-axial Braid $[0/\pm 45]_4$	54.5	43.0	1.419

Table II Carbon fiber plaque composite mechanical properties.

Direction	Stress, Max (MPa)	Modulus (GPa)	Poisson's Ratio	Strain, Max (%)
Tensile				
0°	654	60.33	0.562	1.08
90°	65.2	8.756	0.109	1.20
Compressive				
0°	376	59.71	--	0.66
90°	91.7	10.06	--	0.89
Physical Properties	Density (gm/cm^3)	Fiber Weight Content (%)	Resin Weight Content (%)	
Fiber	1.80			
Resin	1.14			
Composite	1.42	54.74	45.26	

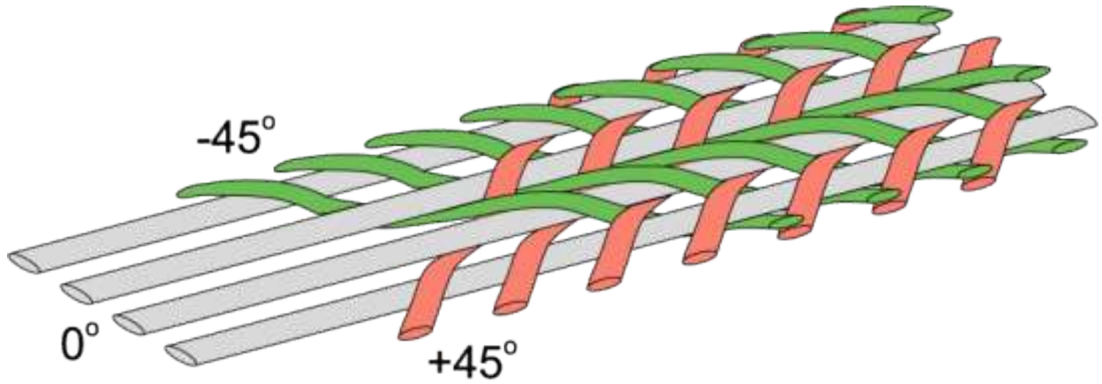

Figure 2 Tri-axial braid schematic.

The strip dimensions are nominally 25.4 mm wide and 200 mm long. One end of each strip is beveled at a 45º angle. The purpose of the bevel to lower the initial load peak and, thus, improve the structural stability of test. This bevel is usually present in composite crush tubes for the same reason. When the strip is compressed, the bevel is oriented away from the roller D, or to the left as shown in Figure 1. A strip test specimen is shown in Figure 3. The strip test fixture with a strip specimen ready to be tested is presented in Figure 4. A typical crushed specimen is presented in 5.

Figure 3 Strip test coupon.

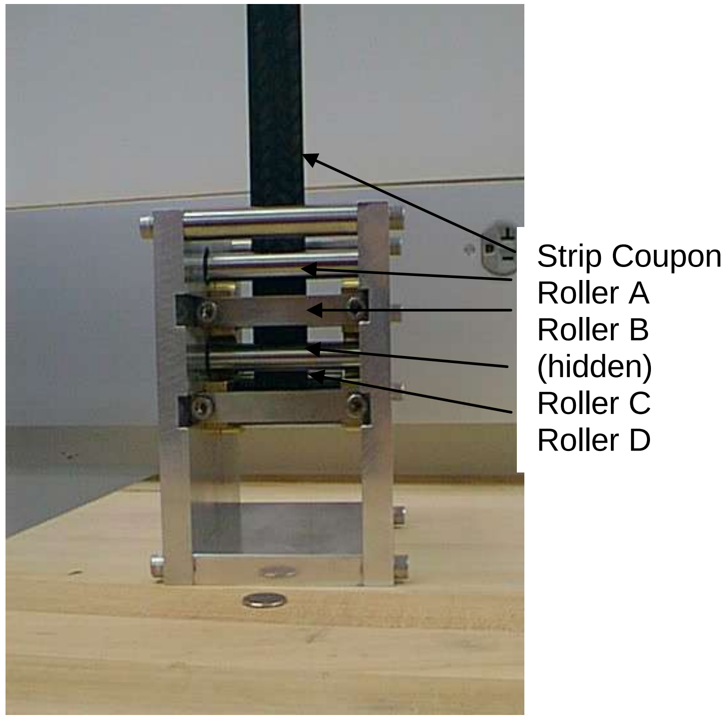

Figure 4 Strip test fixture with coupon.

Figure 5 Typical tested strip coupon.

Quasi-Static Strip Tests

Five strip specimens were quasi-statically (0.0508 m/min) loaded with roller D locked. The results of these tests are presented in Table III. Five additional strip specimens were quasi-statically at the same rate with roller D locked and the strips lubricated with zinc stearate. Zinc stearate is a dry film lubricant used for these tests to show the effect of altering the coefficient of sliding friction between the composite strips and fixed steel roller D. The results of these testes are presented in Table IV. A third set of five strip specimens were quasi-statically (0.0508 m/min) loaded with roller D free to rotate during testing. The results of these testes are presented in Table V.

The load-displacement curve of each test was numerically integrated to calculate the absorbed energy. The calculated absorbed energy was divided by the mass of the portion of the strip that was compressed to determine the SEA for each specimen tested. A typical load-displacement plot is presented in Figure 6. Note that there is a high peak load with load drop-off to a plateau load. No damage to the composite strip occurs until a peak load is achieved at which time the damage process begins in the strip. Once damaged, the load required to create new damage in the tube occurs at a lower level.

Table III Carbon fiber composite strip SEA, locked roller D quasi-static loading (0.0508 m/min).

Coupon	Cross Section Area (cm^2)	Max. Load (N)	Ave. Load (N)	Load Distance (cm)	Total Energy Absorbed (J)	SEA (J/gm)
4374-4-3-V	1.19	7,035	3,414	11.5	391	20.1
4374-4-3-W	1.18	7,201	3,295	11.4	377	19.5
4374-4-3-X	1.05	4,285	2,815	11.4	322	18.8
4374-4-3-Y	1.18	6,115	3,170	11.4	368	18.8
4374-4-3-Z	1.15	7,961	3,147	11.4	360	19.1
Ave.	1.15	6,519	3,168	11.4	364	19.3

Notes: SEA based on material density of 1.42 gm/cm^3.

Table IV Carbon fiber composite strip SEA, locked and lubricated roller D, quasi-static loading (0.0508 m/min).

Coupon	Cross Section Area (cm^2)	Max. Load (N)	Ave. Load (N)	Load Distance (cm)	Total Energy Absorbed (J)	SEA (J/gm)
4374-4-3-AA	1.16	7,344	2,534	11.4	290	15.3
4374-4-3-BB	1.19	6,685	2,553	11.5	292	15.1
4374-4-3-CC	1.16	7,041	2,400	11.5	275	14.5
4374-4-3-DD	1.14	6,973	2,420	11.5	277	14.9
4374-4-3-EE	1.16	6,719	2,273	11.5	260	13.7
Ave.	1.16	6,952	2,436	11.5	279	14.7

Notes: SEA based on material density of 1.42 gm/cm^3.

Strips lubricated with zinc stearate dry film.

Table V Carbon fiber composite strip SEA, free roller D, quasi-static loading (0.0508m/min)

Coupon	Cross Section Area (cm^2)	Max. Load (N)	Ave. Load (N)	Load Distance (cm)	Total Energy Absorbed (J)	SEA (J/gm)
4374-4-3-FF	1.16	5,782	2,133	11.5	244	12.9
4374-4-3-GG	1.16	5,996	2,417	11.5	277	14.6
4374-4-3-HH	1.16	5,887	2,171	11.5	249	13.1
4374-4-3-II	1.16	6,332	2,363	11.5	271	14.3
4374-4-3-JJ	1.13	2,556	1,881	11.5	215	11.7
Ave.	1.15	5,311	2,193	11.5	251	13.3

Notes: SEA based on material density of 1.42 gm/cm^3.

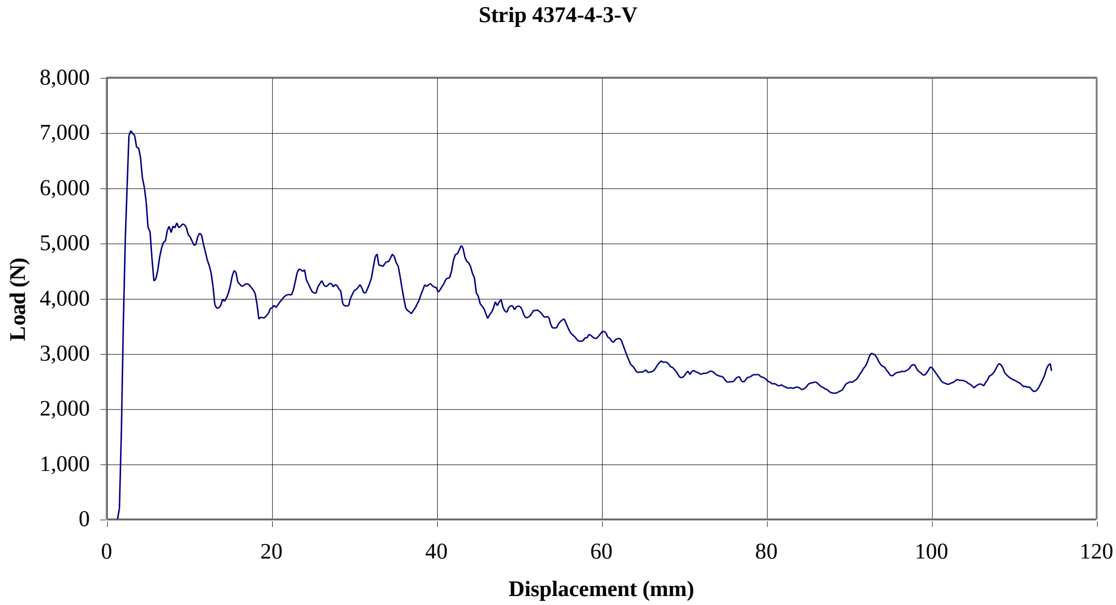

Figure 6 Typical load-displacement plot for quasi-static loaded (0.0508 m/min) carbon composite strip with locked roller D.

Dynamic Strip Tests, Locked Roller D

Five strip specimens were tested dynamically at 2.0 m/sec with roller D locked. Three specimens were tested at 0.5 m/sec with the roller D locked. The results of these tests are presented in Tables VI and VII. There was no significant difference in the SEA of strips tested at 2.0 m/sec and 0.5 m/sec (15.5 J/gm vs. 15.4 J/gm). A plot of a typical load-displacement curve for 2.0 m/sec and 0.5 m/sec loading is presented in Figure 7.

Table VI Carbon fiber composite strip SEA, locked roller D, dynamic loading (2.0 m/sec).

Coupon	Cross Section Area (cm^2)	Max. Load (N)	Ave. Load (N)	Load Distance (cm)	Total Energy Absorbed (J)	SEA (J/gm)
4374-4-3-QQ	1.07	6,607	2,253	10.9	246	16.6
4374-4-3-RR	1.12	8,194	2,429	10.8	263	15.7
4374-4-3-SS	1.11	10,307	2,322	11.0	256	14.6
4374-4-3-TT	1.13	6,882	2,243	10.9	244	13.8
4374-4-3-UU	1.04	5,035	2,513	10.9	275	16.9
Ave.	1.09	7,405	2,352	10.9	257	15.5

Notes: SEA based on material density of 1.42 gm/cm^3.

Table VII Carbon fiber composite strip SEA, locked roller D, dynamic loading (0.5 m/sec).

Coupon	Cross Section Area (cm^2)	Max. Load (N)	Ave. Load (N)	Load Distance (cm)	Total Energy Absorbed (J)	SEA (J/gm)
4374-4-3-BBB	1.08	6,897	2,139	11.1	237	13.9
4374-4-3-CCC	1.12	6,958	2,503	10.9	273	15.6
4374-4-3-DDD	1.08	7,706	2,579	11.0	285	16.7
Ave.	1.09	7,187	2,407	11.0	265	15.4

Notes: SEA based on material density of 1.42 gm/cm^3.

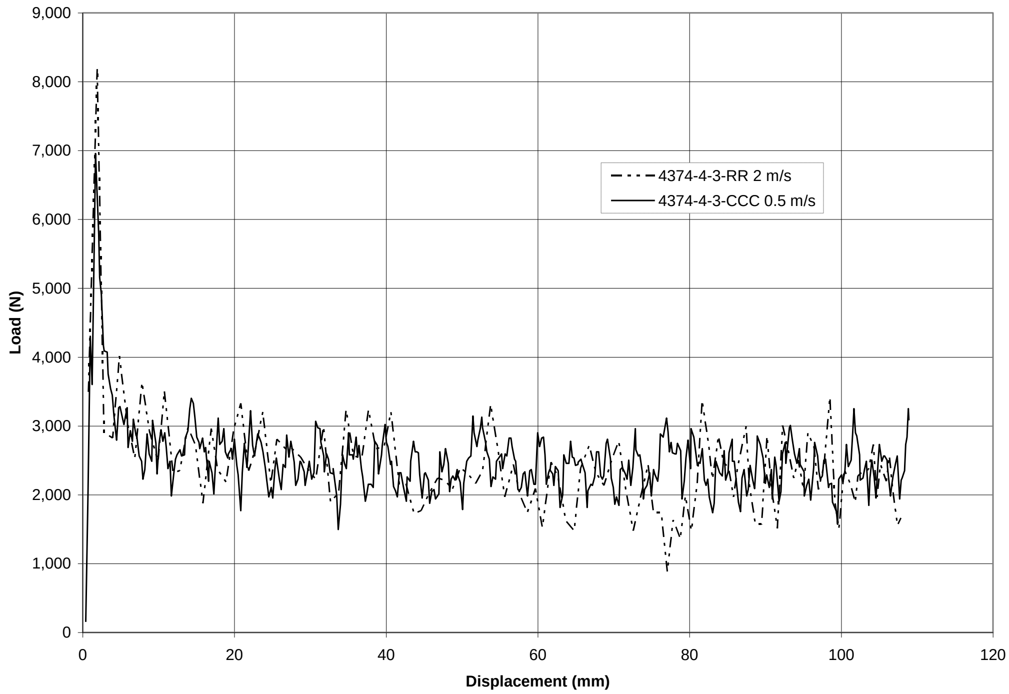

Figure 7 Typical carbon composite strip load-displacement with locked roller D at 2 m/s and 0.5 m/s load rates.

Roller D was locked and specimens were loaded at 2.0 m/sec for the next set of five strip specimens. However, these five strips were coated with zinc stearate to reduce sliding friction. The results of these tests are presented in Table VIII.

Table VIII Typical carbon composite strip load-displacement with locked roller D at 2 m/s and 0.5 m/s load rates.

Coupon	Cross Section Area (cm^2)	Max. Load (N)	Ave. Load (N)	Load Distance (cm)	Total Energy Absorbed (J)	SEA (J/gm)
4374-4-3-VV	1.13	6,592	2,132	10.9	233	13.2
4374-4-3-WW	1.09	8,453	2,095	10.6	222	13.4
4374-4-3-XX	1.10	8,850	2,284	11.0	249	14.6
4374-4-3-YY	1.10	10,468	2,278	11.0	251	14.5
4374-4-3-AAA	1.19	8,835	2,305	10.8	249	14.6
Ave.	1.12	8,640	2,219	10.9	241	14.1

Notes: SEA based on material density of 1.42 gm/cm^3.

Lubricated with zinc stearate dry film.

Dynamic Strip Tests, Roller D Free

The results for dynamic loading of strips with roller D free to rotate are presented in Table IX for 2.0 m/sec and in Table 10 for 0.5 m/sec. The average SEA for 2.0 m/sec and 0.5 m/sec load rates are close in value (13.0 J/gm vs. 13.3 J/gm).

Table IX Carbon fiber composite strip SEA, free roller D, dynamic loading (2.0 m/sec).

Coupon	Cross Section Area (cm^2)	Max. Load (N)	Ave. Load (N)	Crush Distance (cm)	Total Energy Absorbed (J)	SEA (J/gm)
4374-4-3-LL	1.13	6,546	1,934	10.9	210	11.9
4374-4-3-MM	1.13	9,659	2,073	10.9	227	12.8
4374-4-3-NN	1.05	7,706	2,081	10.9	228	13.8
4374-4-3-OO	1.09	7,385	2,170	10.9	237	13.9
4374-4-3-PP	1.10	6,119	2,018	10.9	220	12.8
Ave.	1.10	7,479	2,055	10.9	224	13.0

Note: SEA based on material density of 1.42 gm/cm^3.

Table X Carbon fiber composite strip SEA, free roller D, dynamic loading (0.5 m/sec).

Coupon	Cross Section Area (cm^2)	Max. Load (N)	Ave. Load (N)	Crush Distance (cm)	Total Energy Absorbed (J)	SEA (J/gm)
4374-4-3-EEE	1.05	2,960	1,794	11.0	198	12.0
4374-4-3-FFF	1.09	5,402	2,317	11.1	256	14.8
4374-4-3-GGG	1.09	5,493	2,038	11.1	226	13.1
Ave.	1.08	4,618	2,050	11.1	227	13.3

Note: SEA based on material density of 1.42 gm/cm^3.

Strip Test Results Discussion and Summary

A summary of strip testing is presented in Table XI. The variables presented are: load speed, roller D fixity, and the presence or absence of lubrication. The first comparison can be made for cases with varied load speed, locked roller D, and specimens lubricated or not lubricated with zinc stearate. When the loading is quasi-static (case 1), the average SEA is 19.3 J/m. When the loading is dynamic, either at 2.0 m/sec (case 4) or 0.5 m/sec (case 7), the average SEA is 15.4 J/m, a 20% reduction compared with the quasi-static result.

When the roller D is locked and the strips are lubricated with zinc stearate, the SEA for quasi-static loading (19.3 J/gm of case 1 vs. 14.7 J/gm of case 2) vs. dynamic loading at 2.0 m/sec (14.1 J/gm of case 5). The zinc stearate lubrication resulted in a reduction in SEA of 23.8% (14.7 J/gm of case 2 vs. 19.3 J/gm of case 1) compared with quasi-static loading. However, when tested dynamically at 2.0 m/sec, the reduction in SEA for the lubricated strips was only 8.4% compared with the non-lubricated test strips (14.1 J/gm of case 5 vs. 15.4 J/gm of case 4).

When the roller D is free to rotate there was little difference observed in the SEA between quasi-static loading (13.3 J/gm of case 3) and dynamic load rate of 0.5 m/sec (13.3 J/gm of case 8). There was only a slight difference in SEA when the dynamic load rate is 2.0 m/sec (13.0 J/gm of case 6).

Table XI Strip test results summary.

Case	Crush Speed	Roller D Fixity	Lubrication	Average SEA (J/gm)
1	Quasi-Static	Locked	None	19.3
2	Quasi-Static	Locked	Yes	14.7
3	Quasi-Static	Free	None	13.3
4	2.0 m/sec	Locked	None	15.4
5	2.0 m/sec	Locked	Yes	14.1
6	2.0 m/sec	Free	None	13.0
7	0.5 m/sec	Locked	None	15.4
8	0.5 m/sec	Free	None	13.3

Conclusions

Sliding friction absorbs a significant amount of energy, at least in quasi-static cases.

Altering the coefficient of friction of the composite tube surface can vary SEA.

Energy absorption due to sliding friction can be separated from those due to damage formation.

The decrease in SEA between dynamic and quasi-static loading is due almost entirely to the difference in sliding friction SEA between dynamic and quasi-static loading.

Acknowledgements

The author would like to thank and acknowledge the contributions of the following individuals and organizations for support of this research.

The technical fabricators of the Ford Scientific Research Laboratory shop, Paul Ostrander and Gary Fleming, for the fabrication of and their design suggestions of the strip test fixture.

Mike Starbuck and Rick Battiste of Oak Ridge National Laboratory, National Transportation Research Center, for conducting dynamic load tests.

Dan Houston and Ron Cooper of the Ford Scientific Research Laboratory for performing quasi-static crush tests.

Nancy Johnson and Ruth Gusko of the GM Research Center for plaque fabrication.

I would also like to acknowledge and thank the DOE program management team and the Board and staff of the Automotive Composites Consortium. This work was sponsored by the Automotive Composites Consortium and the U. S. Department of Energy, Office of Transportation Technologies, Office of Advanced Technologies, Lightweight Materials Program under Cooperative Agreement number FC05-02OR22910.